Journal of Exploratory Research in Pharmacology **2023** vol. 8(2) | 95–106
DOI: 10.14218/JERP.2022.00061

Original Article

Virtual Screening of Shuanghuanglian Components for the Binding to the Proteinases of SARS-CoV-2

Yu-Shun Yang[1,2,3*], Dilimulati Ainiwaer[2], Xiao Wang[1], Chao-Yue Wang[1] and Jie Yang[2*]

[1]*Jinhua Advanced Research Institute, Jinhua, China;* [2]*State Key Laboratory of Pharmaceutical Biotechnology, School of Life Sciences, Nanjing University, Nanjing, China;* [3]*Research Center of Sensors and Functional Materials, Hi-Techjig Co. Ltd., Zhenjiang, China*

Received: July 22, 2022 | **Revised:** September 06, 2022 | **Accepted:** October 19, 2022 | **Published online:** November 23, 2022

Abstract

Background and objectives: Coronavirus disease 2019 (COVID-19), a global pandemic disease caused by SARS-CoV2 infection, has existed for nearly three years. However, there are currently only a few therapeutic drugs available. The objective of this study attempted to explore the potential therapeutic actions of Shuanghuanglian, a traditional Chinese medicine, using molecular docking simulation technology.

Methods: The ingredients of Shuanghuanglian and the approved drugs were structurally evaluated. The potential bindings of the individual ingredients in Shuanghuanglian to the PLPro and Mpro of the SARS-CoV2 were evaluated by molecular docking simulation according to the energy parameters. The corresponding binding patterns into each defined site were analyzed. The pharmacokinetics of the individual ingredients were predicted to preliminarily evaluate their oral bioavailability.

Results: There were 482 unique natural products in the categories of fatty acids, aromatic compounds, glycosides, and sterols. The successfully docked rates of the Shuanghuanglian components binding to the PLPro and Mpro were all higher than those of the compounds in the Food and Drug Administration-approved Drug Library. In general, Shuang and Lian took the primary status in providing the top hits via the hydrogen bonds, while Huang acted as an important supplement to the global activity. Though the selected hits faced the common difficulty of polarity, the deglycosylation and the package by the carriers could also be practical to overcome the pharmacokinetic violation.

Conclusions: Shuang and Lian retain the potential ability to interact with the PLPro and Mpro of SARS-CoV2, and other herbs seem to have the potential to be involved.

Keywords: Coronavirus disease 2019; Natural products; Virtual screening; Potential interactions; Traditional Chinese medicine.

Abbreviations: ADME, absorption, distribution, metabolism, and excretion; CoV, coronavirus; FDA, Food and Drug Administration, USA; HSA, human serum albumin; MERS, Middle East respiratory syndrome; MOF, metal-organic framework; Mpro, main protease; PLPro, papain-like protease; RdRP, RNA-dependent RNA polymerase; SARS, severe acute respiratory syndrome; SMILE, simplified molecular input line entry system; TCMSP, traditional Chinese medicine systems pharmacology database and analysis platform; TPSA, topological polar surface area.

***Correspondence to:** Yu-Shun Yang, Jinhua Advanced Research Institute, Jinhua 321019, China. ORCID: https://orcid.org/0000-0001-5424-8202. Tel: +86 25-8968-2572, Fax: +86 25-8968-2572, E-mail: ys_yang@nju.edu.cn; Jie Yang, State Key Laboratory of Pharmaceutical Biotechnology, School of Life Sciences, Nanjing University, Nanjing 210023, China. ORCID: https://orcid.org/0000-0002-5983-6414. Tel: +86 25-8359-4060, Fax: +86 25-8359-4605, E-mail: yangjie@nju.edu.cn

How to cite this article: Yang YS, Ainiwaer D, Wang X, Wang CY, Yang J. Virtual Screening of Shuanghuanglian Components for the Binding to the Proteinases of SARS-CoV-2. *J Explor Res Pharmacol* 2023;8(2):95–106. doi: 10.14218/JERP.2022.00061.

Introduction

It has been nearly three years since the Coronavirus (CoV) disease 2019 (COVID-19) was first detected in December 2019 in Wuhan, Hubei Province, China.[1] COVID-19 was caused by an infection with a new CoV named severe acute respiratory syndrome coronavirus 2 (SARS-CoV-2),[2] which was the third highly pathogenic virus in addition to the SARS-CoV in 2003,[3] and the Middle East respiratory syndrome coronavirus (MERS-CoV) in 2012.[4] COVID-19 spread to all countries around the world and was declared a pandemic disease by the World Health Organization.[5,6] The SARS-CoV-2, particularly for the recent dominant Omicron strains, seems to be less fatal (~5% *vs.* ~10% and ~40%, respectively) but is more contagious (R_0 = 2.0–6.5) than SARS and MERS.[7–10] Currently, there are a few drugs that have been approved for the treatment of COVID-19 although different types of vaccines have demonstrated to limit the severity of COVID-19 around the world. Hence,

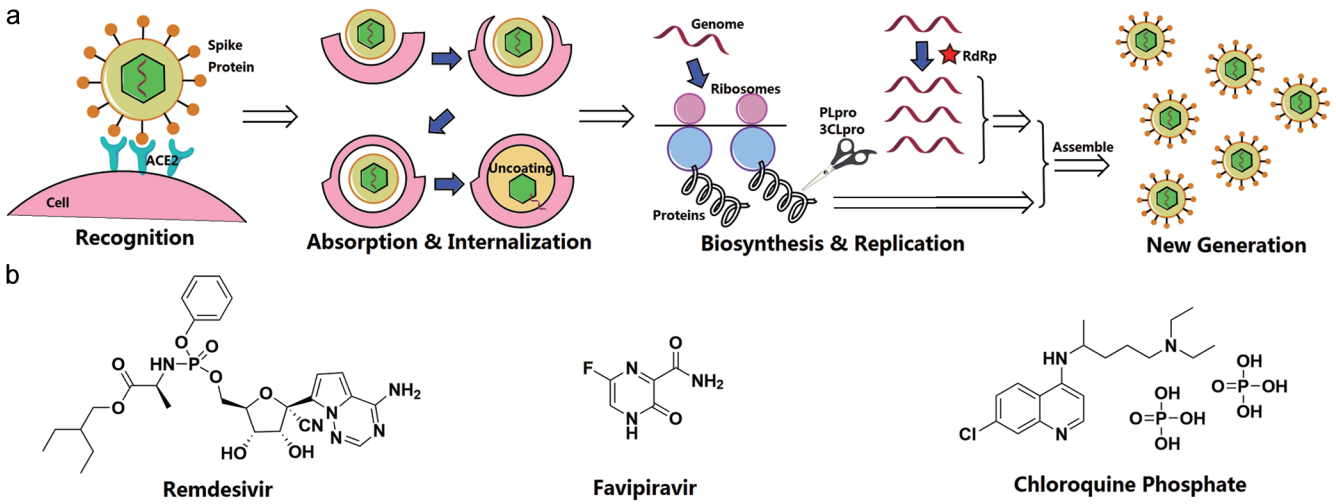

Fig. 1. The life cycle of the SARS-CoV-2 and current potential drugs for COVID-19. (a) The illustration of the SARS-CoV-2 life-cycle following its infection. (b) The potential drugs for treating COVID-19.

understanding the molecular pathogenesis of COVID-19 and the discovery of new therapies are urgently needed (Fig. 1).[11–13] During the life cycle of SARS-CoV-2, four major proteins have been regarded as the potential targets, including the Spike protein for the recognition onto the host, the RNA-dependent RNA polymerase (RdRP) for the replication of RNA, the papain-like protease (PL-Pro), and main protease (Mpro) for preparing the biosynthesis of the next generation of the virus.

At present, the highly restricted policies, immediate isolation of individuals with a positive SARS-CoV2 infection and extensive screening, as well as effective therapies have controlled the spreading of COVID-19 in China.[14,15] In 2020, potential drug candidates, such as Remdesivir, Favipiravir and Chloroquine/Hydroxychloroquine, were chosen for the treatment of COVID-19 patients.[16–19] Recently, Paxlovid and Molnupiravir were approved by the Food and Drug Administration (FDA) of the USA for treatment of patients with early stages of COVID-19 and other biological drugs, such as specific neutralization antibodies that had also been approved for the treatment of patients with severe COVID-19.[20–22] Furthermore, Chinese medicinal herbs, such as Shuanghuanglian, Lianhua Qingwen capsules, Qingfei Paidu decoction, and other modified prescriptions have been recommended for the treatment of patients with mild COVID-19.[16,23,24] However, the pharmacological actions of these Chinese medicinal herbs, particularly for Shuanghuanglian, the first recommended Chinese medicinal herb, have not yet been clarified.[25]

This study explored the potential bindings of the ingredients in Shuanghuanglian to the PLPro and Mpro of SARS-CoV2 according to their crystal structures available in the literature.[26] Shuanghuanglian contains three major ingredients: *Lonicerae Japonicae Flos* (Shuang means Shuanghua also called honeysuckle), *Scutellariae Radix* (Huang means Huangqin), and *Forsythiae Fructus* (Lian means Lianqiao).[27–29] A previous study has reported that miR2911 in honeysuckle inhibits the SARS-CoV-2 replication and accelerates the negative conversion of infected patients.[30–32] Accordingly, we attempted to explore the therapeutic potential of abundant natural products in Chinese medicinal herbs.[33–35] Based on its therapeutic efficiency, the relatively clear compositions, available reference value of other prescriptions, and our previous experience, Shuanghuanglian was chosen for the *in silico* analysis. We scanned the database of the traditional Chinese herbs, analyzed the natural products of each ingredient, conducted the molecular docking simulation, and gave further discussion on the practical potential. Our findings could aid in the design of new medical herbs and help in internationally standardized research on traditional Chinese medicines.[36–38]

Materials and methods

General system and software information

The investigation was mainly conducted on a workstation with the following system configurations: Intel CORE i7-9800X CPU @3.80 GHz processor, system memory: 32 GB RAM, system type: 64-bit operating system, and Windows 10 as the operating system. The data library was mainly summed up and analyzed by the *in silico* simulation in the Windows system using Python and Cygwin. The two-dimensional structure of the compounds was drawn using Chemdraw 14.0 software (ChemBioOffice, CambridgeSoft). The preparation and molecular docking simulation were performed using Discovery Studio 3.5 and Discovery Studio Visualizer 2016 (Accelrys Software, Inc).

Selection of the natural products

The natural products of the corresponding herbs were obtained from the traditional Chinese medicine systems pharmacology database and analysis platform (TCMSP) Version 2.3 launched by the Lab of Systems Pharmacology at Northwest University, Xi'an, Shaanxi Province, China.[39] All the compounds were collected with the Mol ID in this database. The structures in the mol2 format were identified using Chemdraw 14.0 software (ChemBioOffice, CambridgeSoft). The comparison on the percentage of the pass was performed using the FDA-approved Drug Library (2,747 compounds) supported by Selleck (China) (Shanghai, China).

Ligand preparation

All the compounds were prepared with the "Prepare Ligands" modules in Discovery Studio 3.5 (Accelrys Software, Inc). Each prepared ligand was identified to confirm that the conformation agreed with the one in the original database.

Receptor preparation

Based on the topic of the specific treatment instead of the prevention or broad-spectrum therapy, we mainly investigated PLPro and Mpro for preparing the biosynthesis of the next generation virus in the life cycle of SARS-CoV-2. To avoid the same nationality of the initial report,[26] the recent released protein structures by the National Institutes of Health, Bethesda, Maryland, USA or National Science Foundation, Alexandria, Virginia USA were used. Accordingly, the crystal structures of the wild type SARS-CoV-2 PLPro (PDB code: 7JRN),[40] and SARS-CoV-2 Mpro (PDB code: 7CWC) were chosen.[41] Subsequently, we prepared the protein structures with the "Prepare Protein" modules in Discovery Studio 3.5 (Accelrys Software, Inc). During the automatic procedure, the water molecules were eliminated if they did not participate in the interactions, the polar hydrogen was added, and the incomplete loops were repaired. The preparation was performed under a CHARMm minimization.[42]

Afterwards, the hierarchy view of the prepared proteins was unfolded. For PLPro, the binding site was defined as one of GRL0617 (a selective inhibitor of SARS-CoV PLPro).[43] For Mpro, the definition of the binding sites was more complex according to our findings. Basically, the most important site was the N3-binding site as reported.[26] When we studied the receptor cavities more carefully, we defined five binding sites which were more suitable for small molecules. All the binding sites were investigated in this work. Among them, Sites I and II were separated from the N3-binding site, which was near the α-helix-rich region of Mpro; Sites III and IV were independent on the beta (β)-sheet-rich region; while Site V was at the linking position of the two regions.

Molecular docking simulation protocol

Molecular docking simulation was carried out using Discovery Studio 3.5 (Accelrys Software, Inc), and visualization was performed using Discovery Studio Visualizer 2016 (Accelrys Software, Inc). Since the involved ligands bore structural diversity, we chose the graphical user interface CDOCKER protocol, a CHARMm force field-based molecular docking tool with a half-flexible receptor, to implement the simulation.[44] The major steps were as follows:

1. Initially, the conformations of the ligands were generated through high temperature molecular dynamics with different random seeds.
2. In each defined binding site, the original ligands were removed. Subsequently, translating the center of each ligand to a specified position within the receptor active site and performing a series of random rotations led to random orientations of the conformations. During the generation of the random orientations, each time when the calculated softened energy was lower than the set limit, the orientation was recorded. This step was repeated until the desired number (here we set three to improve the accuracy as well as to avoid unnecessary crosses in order) of the low-energy orientations was achieved, or the test times of the bad orientations had reached the maximum number.
3. Afterwards, each recorded orientation was subjected to simulated annealing molecular dynamics. The simulation experienced a heated process and was cooled down to the target temperature. The final energy minimization of each ligand in the rigid receptor using non-softened potential was conducted. The heating steps were 2,000 with 700 of the heating target temperature; while the cooling steps were 5,000 with 300 cooling target temperature.
4. Finally, the CHARMm energy (interaction energy plus ligand strain) and the interaction energy alone of each recorded pose were calculated. Three (as we set) poses saved for each ligand were ranked according to the CHARMm energy and the dock scores (more negative, thus more favorable for binding).

Pharmacokinetic properties and Lipinski's rule of five

The pharmacokinetic properties comprising absorption, distribution, metabolism, and excretion (ADME) were predicted using the Swiss ADME protocol (http://www.swissadme.ch/).[45,46] The predicted data from this source were checked with the data from the TCMSP Version 2.3.[39] We also checked the top hits with the Lipinski's oral drug likeliness properties consisting of: 1) the molecular weight (<500 Daltons), 2) number of hydrogen bond donors (<5), 3) number of hydrogen bond acceptors (<10), 4) log P (<5), and 5) molar refractivity (<140).[47]

Results and discussion

Preliminary analysis of the natural products

Shuanghuanglian contained three major ingredients: *Lonicerae Japonicae Flos* (Shuang), *Scutellariae Radix* (Huang), and *Forsythiae Fructus* (Lian). The natural products of the corresponding herbs were obtained from the TCMSP system Version 2.3.[39] From this database, the structures were downloaded and named with their Mol ID. In Table S1, the Mol ID of the compounds from all three herbs were listed. A general analysis of these natural products led to some hints. First, the reported number of natural products in Shuang, Huang, and Lian were 236, 143 and 150, respectively. They were all rich in diversity because a random sampling of 10 herbs in the database indicated that all 10 herbs had fewer than 50 natural products. Secondly, some of the components of the herbs were repeated. As colored in Table S1 and shown in Figure 2, 20 compounds in Shuang and Huang, 21 compounds in Shuang and Lian, 10 compounds in Huang and Lian, were the same. There were four compounds (MOL000069, MOL000254, MOL000357, and MOL000358) that appeared in all three herbs. Interestingly, they covered the categories of fatty acids, aromatic compounds, glycosides, and sterols. Moreover, there were 482 distinguished natural products in Shuanghuanglian.

Molecular docking simulation

Focusing on specific treatment, we chose the crystal structures of the wild type SARS-CoV-2 PLPro (PDB code: 7JRN),[40] and SARS-CoV-2 Mpro (PDB code: 7CWC),[41] respectively. For the other two enzymes, because the Spike protein might be for prevention and RdRP for the broad-spectrum treatment, which could also be helped by miR2911,[32] the binding sites of the PLPro and Mpro were identified. As shown in Figure 3, the binding site in PLPpro was that of the original ligand GRL0617, while the binding sites in Mpro were complex. The basic site was that of ligand N3 together with another five binding sites. Sites I and II were separated from the N3-binding site, which was near the alpha (α)-helix-rich region of the Mpro; Sites III and IV were independent in the β-sheet-rich region, while Site V was at the linking position of the two regions. All of the natural products could have binding sites according to the steric and electronic surroundings. We chose the CDOCKER protocol considering the structural diversity of the ligands. Accordingly, the "-CDOCKER Interaction Energy" was selected as the basic index to evaluate the possibility of the interaction between each ligand and the binding site, while the "-CDOCKER Energy" was chosen as the reference index to evaluate the possible steadiness of the ligand-receptor complex.

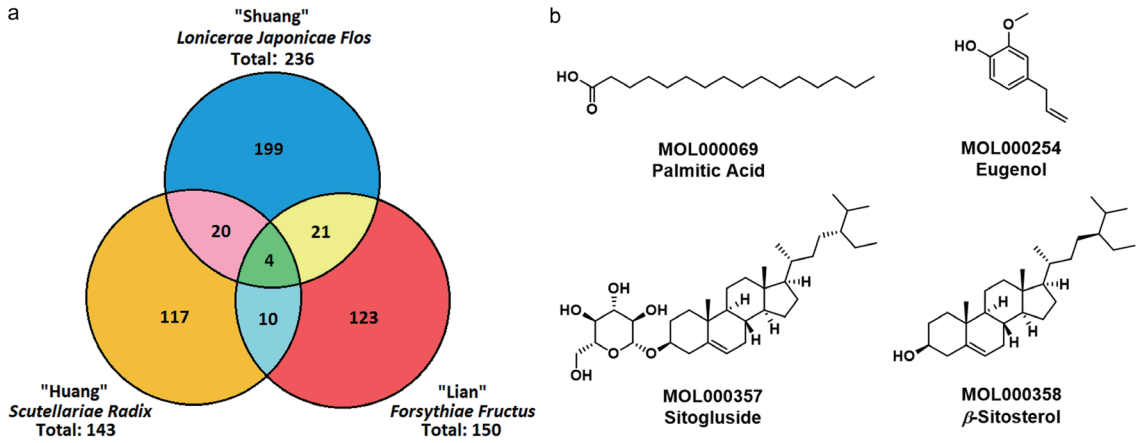

Fig. 2. The number of ingredients in Lonicerae Japonicae Flos (Shuang), Scutellariae Radix (Huang), and Forsythiae Fructus (Lian), and four compounds in all three herbs. (a) The numbers of natural products in the three herbs. (b) The compounds that appeared in all three herbs.

From the simple object to the complex one, we chose to analyze the results from SARS-CoV-2 PLPro. Among the 482 natural products, 438 were docked into this site while 255 reached the basic requirement of potential interactions (we set as -CDOCKER Interaction Energy >30.0 kcal/mol). We listed the MOL IDs of the 255 compounds in Table S2 and illustrated the 2D binding patterns of the top 15 hits in Figure S1. The top 15 hits were also compared in Table 1. First, Shuanghuanglian seemed to have potential for SARS-CoV-2 PLPro because 90.87% (438 out of 482) of its investigated components were docked into the PLPro, which was higher than that of the compounds in the FDA-approved Drug Library supported by Selleck (China) (Shanghai, China) (81.14%; 2,229 out of 2,747). Simultaneously, the "-CDOCKER Interaction Energy" of the top hits were almost in the rational range of 40.0–60.0 kcal/mol, which was almost the most potential situation of CDOCKER before further modification and evaluation. Secondly, the flavones, glycosides, and polyphenols were preferred in the top hits, while long chain fatty acid esters also appeared. Specially, among the top hits, long chain fatty acid esters were all from Huang. Thirdly, Shuang and Lian were more important than Huang for binding to the PLPro. Additionally, the repeated compounds did not appear frequently (two out of 15; 13.33%). In particular, as shown in the 3D binding pattern of MOL003130 (Fig. 4a) and MOL002037 (Fig. 4b), the major key residues for the hydrogen bonds were Lys157, Leu162, Asp164, Arg166, Glu167, Gly266, Asn267, Tyr268, Gln269, Tyr273, and Thr301, respectively. We then chose the top three to evaluate their possible druggability.

Actually, with higher homology with SARS-CoV, Mpro has been widely investigated.[26] Here, we also analyzed the results in the N3-binding site before that of the further defined ones. Among the 482 natural products, 451 were docked into this site, while 246 could be potential for interactions with the Mpro. We listed the MOL ID of the 246 compounds in Table S3 and illustrated the 2D binding patterns of the top 15 hits in Figure S2. The hints from the docking results in SARS-CoV-2 Mpro were different (Table 2). Initially, compared with that in PLPro, the success rate of docking was even as high as 93.57% (451 out of 482), which was also higher than that of the compounds in the FDA-approved Drug Library (83.25%; 2,287 out of 2,747). However, one questionable point was that the "-CDOCKER Interaction Energy" of the top hits was all beyond 60.0 kcal/mol, thus suggesting that the N3-binding site could be too large for the investigated ligands. Accordingly, we subsequently divided it into smaller sites. Secondly, flavones, glycosides, and polyphenols were preferred. Simultaneously, the long chain species were alkanes. The long chain compounds were all from Huang, and they were not favorable for generating hydrogen bonds. Thirdly, though Shuang and Lian still covered a majority of the top hits, their compounds were quite different from those

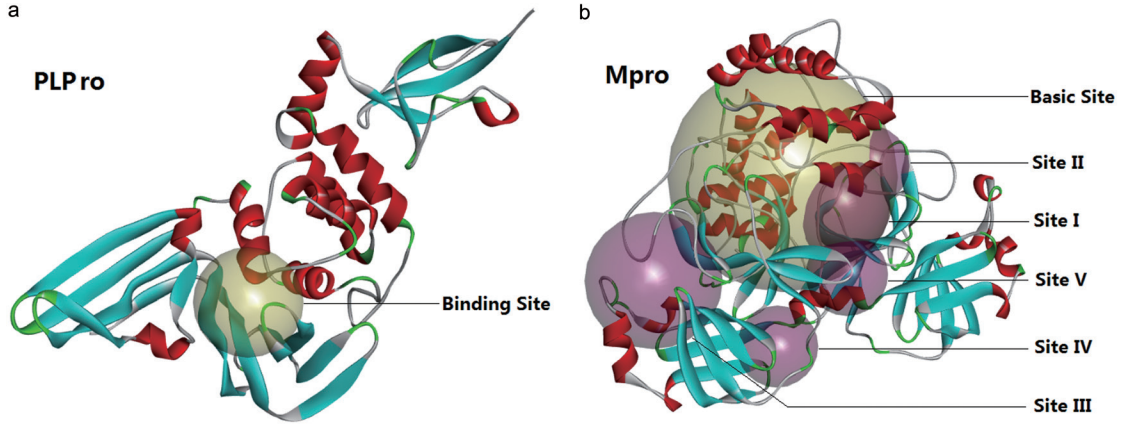

Fig. 3. The defined binding sites in SARS-CoV-2 PLPro (a) and Mpro (b). Mpro, main protease; PLPro, papain-like protease.

Table 1. The comparison of the top 15 hits in SARS-CoV-2 PLPro

MOL ID	-CDOCKER interaction energy (kcal/mol)	-CDOCKER energy (kcal/mol)	Source	Number of H-bonds	General name
MOL003130	−6.29035	63.3313	Shuang	10	Madreselvin A
MOL002037	41.0151	60.9759	Lian	7	Amentoflavone
MOL000010	−3.98465	58.1761	Shuang	7	Rhoifolin
MOL001875	44.3396	57.8812	Shuang	4	Isochlorogenic acid
MOL003051	−1.68697	56.8953	Shuang	1	Scolymoside
MOL003309	38.3745	56.5246	Lian	6	Plantainoside A
MOL003076	35.8932	56.4097	Shuang	2	3,5-Di-O-caffeoylquinic acid methyl ester
MOL003284	31.5003	56.2757	Lian	5	Caleolarioside A
MOL003077	38.4369	56.182	Shuang	8	4,5-Di-O-caffeoylquinic acid methyl ester
MOL003334	−3.93747	55.5806	Lian	7	Forsythoside D
MOL000415	−2.95525	55.0801	Shuang & Lian	3	Rutin
MOL013161	51.9647	54.8761	Huang	1	Methyl Hexacosanoate
MOL007792	8.65799	54.3395	Huang	4	Isomartynoside
MOL009734	49.455	53.8073	Huang	1	Methyl lignocerate
MOL000007	14.4816	53.6873	Shuang & Huang	4	Cosmetin

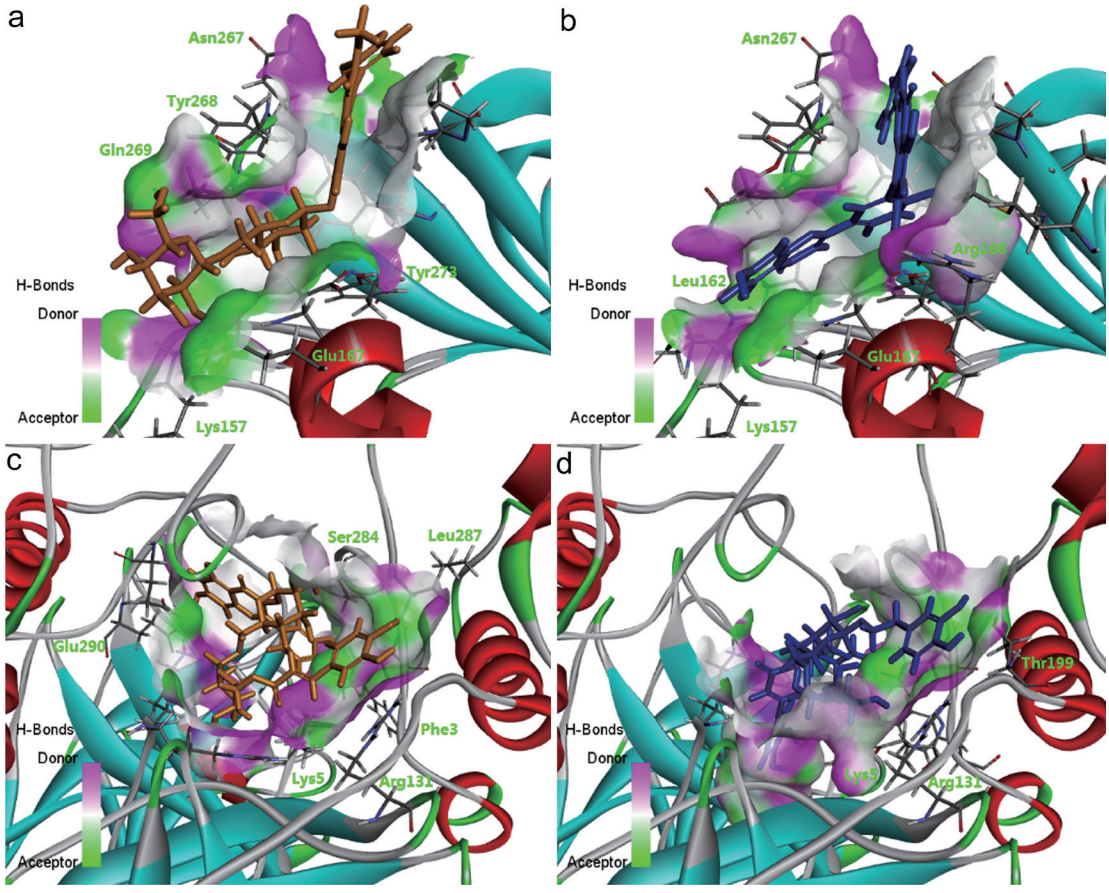

Fig. 4. The 3D binding patterns of the top hits in the detailed binding sites with the H-bond surface comprising MOL003130 in PLPro (a), MOL002037 in PLPro (b), MOL003008 in Mpro (c), and MOL003337 in Mpro (d).

Table 2. The comparison of the top 15 hits in SARS-CoV-2 Mpro at the N3-binding site

MOL ID	-CDOCKER interaction energy (kcal/mol)	-CDOCKER energy (kcal/mol)	Source	Number of H-bonds	General name
MOL003008	17.0653	74.3945	Shuang	9	Madreselvin B
MOL003337	13.6612	74.0027	Lian	6	Forsythoside F
MOL003332	29.1808	71.6769	Lian	7	Forsythoside C
MOL003110	−52.6021	71.2342	Shuang	5	Centauroside
MOL003130	0.355922	68.1028	Shuang	7	Madreselvin A
MOL000870	54.4467	64.6227	Huang	0	Hexatriacontane
MOL007792	20.8246	63.9904	Huang	5	Isomartynoside
MOL003331	24.3554	63.6139	Lian	4	Forsythiaside
MOL003285	−5.4399	63.3833	Lian	9	N/A
MOL003333	27.1839	62.5565	Lian	7	Acteoside
MOL003316	28.799	61.8015	Lian	5	*β*-Hydroxyacteoside
MOL003013	12.6776	61.1352	Shuang	4	Secologanic dibutylacetal
MOL003313	13.6329	60.7986	Lian	4	Suspensaside A
MOL000522	14.5554	60.2791	Lian	4	Arctiin
MOL005224	57.0222	60.1095	Huang	0	Tetratetracintane

docked in the PLPro because only two out of 15 (MOL003130 and MOL007792) were the same. All the top hits were unique herbs. We illustrated the 3D patterns of MOL003008 (Fig. 4c) and MOL003337 (Fig. 4d) to infer the key residues for the hydrogen bonds as Phe3, Arg4, Lys5, Arg131, Thr199, Ser284, Leu287, Glu288, and Glu290, respectively.

In addition, it could be possible that smaller binding sites could be more rational than the N3-binding site for the prepared ligands. Instead of simply reducing the radius, we identified the new sites according to the real cavities. Preliminarily, we compared the feasibility of the five divided sites. The successful docked and interaction possible ligands were Site I: 339 and 21; Site II: 436 and 257; Site III: 390 and 173; Site IV: 367 and 169; Site V: 412 and 221. Because the top hit (MOL003283) in Site I indicated the "-CDOCKER Interaction Energy" of merely 36.0175 kcal/mol, we reasonably believed that Site I did not have the potential for the prepared ligands from Shuanghuanglian. The top 50 hits in each site were listed in Table S4, and the 2D binding patterns of the top 15 hits were illustrated in Figures S3-S6. Site II was similar too, but smaller than the N3-binding site. From the energy index in Table 3, Site II was also more rational than the N3-binding site, which realized our purpose of defining the divided sites. The top hits were all formed from flavones, glycosides, and polyphenols. Shuang and Lian contributed to 14 out of 15 top hits, except the one that appeared in both herbs. Since Site II was similar to the N3-binding site, a high percentage of ligands (33.3%, five out of 15, were marked in Table 3) appeared in the top hits in both sites. We compared the detailed binding patterns of MOL003130 in both sites (Fig. 5a, b, and d), and found that these two conformations interacted with the different residues in the Mpro. Coincidently, MOL003130 also appeared in the top hits in PLPro. Other repeated ligands in both the Mpro Site II and PLPro included MOL000415, MOL001875, MOL003051, MOL000010, and MOL003334. For each repeat, we picked the top three from the previously unpicked ones for further evaluation. They were MOL003316, MOL003313, MOL003013, MOL000415, MOL001875, and MOL003051.

When we divided the sites, we thought that Sites III and IV were not typical for the small molecular ligands because they were surrounded mainly by the *β*-sheet and their successfully docked ligands were relatively fewer (<400). Though the energy index was also less favorable, these two sites could have potential because the "-CDOCKER Interaction Energy" of the top hits was almost in the rational range of 40.0–60.0 kcal/mol (Tables 4 and 5). Interestingly, the compounds from Huang, regardless of their chain lengths, appeared more frequently in the top hits. Accordingly, we could not ignore the possibility that Huang might interact at these binding sites and act as an important supplement to the overall activity of Shuanghuanglian.

Although the surrounding of Site V contained both the *α*-helix and *β*-sheet, the top hits seemed more similar to the ones in Site II, which were in an *α*-helix-rich region. As shown in Table 6, four out of the top five hits (in total five out of 15 as marked) repeated the top hits in Site II or the N3-binding site. We noticed that MOL003130 appeared again in the leading position with the potential energy values. Given that Site V was close to the N3-binding site, we illustrated the detailed binding patterns of MOL003130 in Site V (Fig. 5c) and compared its relative position in Mpro (Fig. 5d). Because these two conformations were both bound near the center of the corresponding sites, there seemed no key residues to interact with both of the conformations of MOL003130. Alternatively, MOL003130 could bind to the different sites of the Mpro simultaneously. We also selected the top three unpicked ligands from this site (MOL003336, MOL003284, and MOL003334).

Pharmacokinetic potential

We picked 15 hits to predict their pharmacokinetic potential by checking the ADME properties and the violation with Lipinski's rule of five. The major properties were listed in Table S5 with the corresponding simplified molecular input line entry system

Table 3. The comparison of the top 15 hits in the SARS-CoV-2 Mpro Site II

MOL ID	-CDOCKER interaction energy (kcal/mol)	-CDOCKER energy (kcal/mol)	Source	Number of H-bonds	General name
MOL000415	6.83568	64.3218	Shuang & Lian	11	Rutin
MOL003130	−8.23777	63.2077	Shuang	8	Madreselvin A
MOL001875	34.2741	61.9011	Shuang	7	Isochlorogenic acid
MOL003051	1.79757	61.1418	Shuang	7	Scolymoside
MOL002921	11.635	59.2781	Huang	9	N/A
MOL003316	21.7516	59.1990	Lian	7	*β*-Hydroxyacteoside
MOL000010	5.53976	59.0876	Shuang	6	Rhoifolin
MOL003118	37.2258	58.1035	Shuang	9	Isochlorogenic acid C
MOL003332	15.5971	58.0757	Lian	5	Forsythoside C
MOL003334	12.9183	56.2545	Lian	8	Forsythoside D
MOL006370	30.5446	55.3136	Huang	7	5-O-Caffeoylquinic acid
MOL003313	4.35655	55.2171	Lian	4	Suspensaside A
MOL003013	−17.4498	55.1203	Shuang	3	Secologanic dibutylacetal
MOL003010	22.1107	54.5034	Shuang	6	Quercetin-3-O-*β*-D-glu
MOL003336	15.8194	53.9310	Lian	8	Forsythoside E

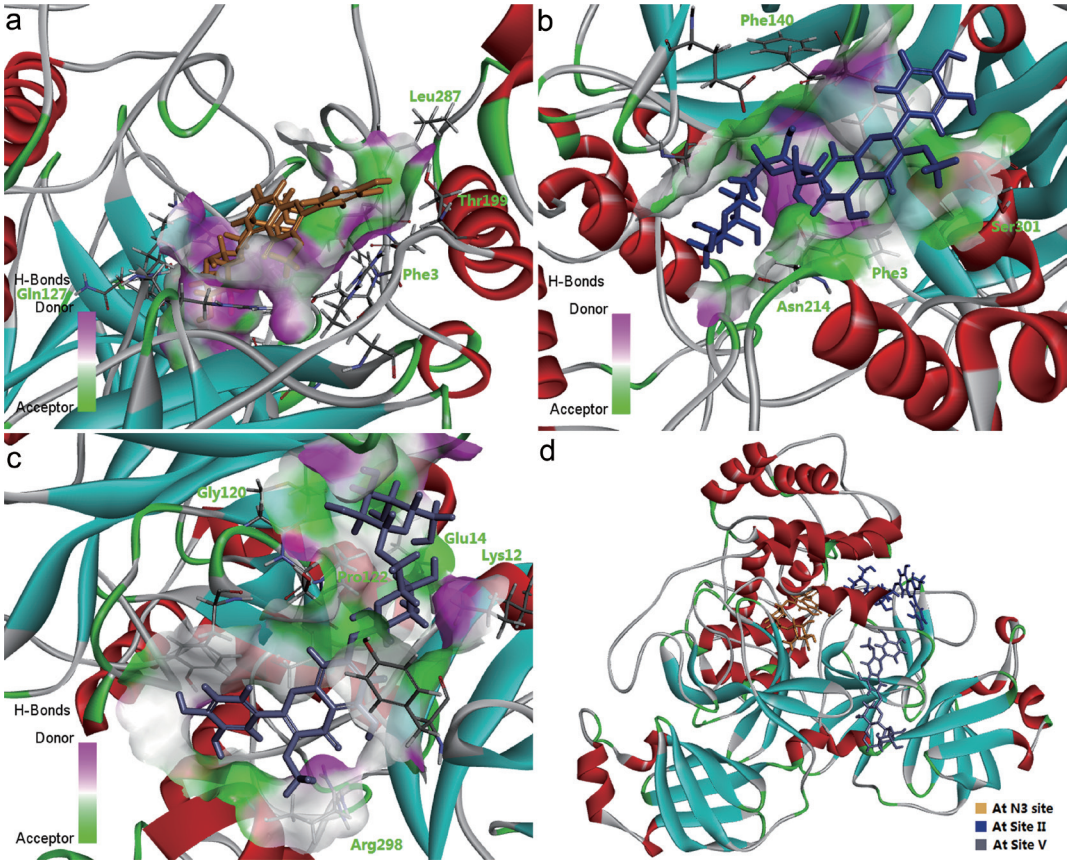

Fig. 5. The 3D binding patterns of MOL003130 to SARS-CoV-2 detailed in the N3-binding site (a), Sites II (b) and V (c), and in the relative positions of the above sites (d).

Table 4. The comparison of the top 15 hits in the SARS-CoV-2 Mpro Site III

MOL ID	-CDOCKER interaction energy (kcal/mol)	-CDOCKER energy (kcal/mol)	Source	Number of H-bonds	General name
MOL000870	42.1147	48.0156	Huang	0	Hexatriacontane
MOL008595	42.8505	46.4620	Huang	1	Methyl henicosanoate
MOL005368	41.4543	45.0270	Huang	2	Methyl tricosanoate
MOL003284	27.3505	44.9463	Lian	3	Caleolarioside A
MOL003290	19.0479	44.4435	Lian	3	N/A
MOL003010	16.5869	43.5525	Shuang	6	Quercetin-3-O-*β*-D-glu
MOL000702	10.2468	43.2031	Lian	5	Guajavarin
MOL009730	29.8744	42.6731	Huang	1	Methyl icos-11-enoate
MOL000663	43.3447	42.6685	Shuang	1	Lignoceric acid
MOL002879	41.0219	42.5431	Huang	1	Diop
MOL003322	−1.69405	42.5174	Lian	4	Forsythinol
MOL005224	31.3177	42.3766	Huang	0	Tetratetracintane
MOL002027	38.0839	42.3339	Huang	0	Methyl behenate
MOL003030	33.7532	42.3317	Shuang	0	Ginnol
MOL002934	16.9542	42.2364	Huang	5	Neobaicalein

(SMILES) codes in Table S6, and the oral bioavailability radar maps were presented in Figure 6. For treating COVID-19, we analyzed the oral bioavailability. For all of the selected hits, all the natural products had the most common difficulty of polarity. Given the major structural moieties were flavones, glycosides, and polyphenols, their topological polar surface area (TPSA) went beyond the limit of 130 $Å^2$.[48] Moreover, a majority of the hits faced the problem of size (11 out of 15), which could result from the fact that these compounds contained one or more glycosides. Several hits needed improvement on flexibility (five out of 15). Actually, two possible approaches could be applied to improve the oral bioavailability. One was modifying the deglycosylated metabolites of these natural products. As shown in Figure 6, deglycosylated MOL003130 exhibited no violations of Lipinski's rules. Further modification could improve the potential of the interaction with its targets in the binding sites. The others were packaging the drug-like compounds in certain carriers, such as human serum albumin (HSA), metal-organic framework (MOF),

Table 5. The comparison of the top 15 hits in the SARS-CoV-2 Mpro Site IV

MOL ID	-CDOCKER interaction energy (kcal/mol)	-CDOCKER energy (kcal/mol)	Source	Number of H-bonds	General name
MOL003309	32.9477	55.5423	Lian	6	Plantainoside A
MOL000009	18.7637	51.3359	Shuang	5	Luteolin-7-O-glucoside
MOL003345	13.0808	50.3323	Lian	5	N/A
MOL000561	15.2567	50.2364	Shuang & Lian	4	Astragalin
MOL000437	15.4088	49.6075	Lian	5	Hirsutrin
MOL000007	15.1167	49.0453	Shuang & Huang	5	Cosmetin
MOL002935	15.7847	48.0702	Huang	4	Baicalin
MOL002912	22.8402	47.9820	Huang	3	Dihydrobaicalin
MOL002931	25.8930	47.8252	Huang	4	Scutellarin
MOL003284	30.3906	46.1796	Lian	4	Caleolarioside A
MOL003297	−5.35172	46.0809	Lian	3	N/A
MOL003010	18.5803	45.6709	Shuang	6	Quercetin-3-O-*β*-D-glu
MOL000702	9.11693	44.8240	Lian	3	Guajavarin
MOL003128	2.8717	44.7907	Shuang	3	Dinethylsecologanoside
MOL003119	−8.58632	44.5271	Shuang	6	Loniceracetalide A

Table 6. The comparison of the top 15 hits in the SARS-CoV-2 Mpro Site V

MOL ID	-CDOCKER interaction energy (kcal/mol)	-CDOCKER energy (kcal/mol)	Source	Number of H-bonds	General name
MOL003130	−3.17177	62.6809	Shuang	6	Madreselvin A
MOL003336	−3.49283	57.1383	Lian	7	Forsythoside E
MOL003284	34.4530	56.6149	Lian	8	Caleolarioside A
MOL003334	2.75989	55.4900	Lian	8	Forsythoside D
MOL003285	−13.2275	54.0015	Lian	4	N/A
MOL000536	13.0390	53.3301	Lian	3	Matairesinoside
MOL003309	31.5105	52.9643	Lian	6	Plantainoside A
MOL002702	49.0094	52.6923	Shuang	1	Nonacosanol
MOL003030	48.1793	52.3531	Shuang	2	Ginnol
MOL003020	7.01853	51.5526	Shuang	3	Secologanoside 7-methylester
MOL003118	31.1981	51.4023	Shuang	6	Isochlorogenic acid C
MOL009734	50.1233	51.1693	Huang	1	Methyl lignocerate
MOL003327	17.7518	51.0608	Lian	5	Rengyoside C
MOL000357	−50.5619	50.5453	All	2	Sitogluside
MOL003292	−11.9878	50.4217	Lian	3	(+)-Epipinoresinol-4′-O-D-glucoside

and aptamers. Consequently, it could be practical to overcome one or two violations.

Future directions

Similarity in the compounds and ingredients

There were some common compounds among the top hits in the different binding sites, including MOL003130, MOL000415, MOL 001875, MOL003051, MOL000010, and MOL003334. They shared some similar moieties, such as phenylpropanoids, flavones, and glycosides. Their ADME properties had advantages in insaturation and flexibility, as well as disadvantages in size and polarity.

Among the relevant efficacious Chinese medicines, there was also similarity in the ingredients. Lianhua Qingwen capsules, supplied during the COVID-19 pandemic in Shanghai in 2022, shared the major ingredients of Shuang and Lian, while Qingfei Paidu decoction shared the major ingredient of Huang.[49,50] Moreover, the involved ingredients, such as *Atractylodes macrocephala* Koidz, *Belamcanda chinensis* (L.) Redouté, and *Citrus reticulata* Blanco, contained similar components as those found in Shuanghuanglian.

Significance of the components and substitutability

Subsequently, we intended to define the sites in the Mpro, especially the separation of Sites I and II. According to the experience of the structural analysis, the analysis of the released structure of Mpro revealed the reported binding site was bulky. The so-called N3-binding site was bound with a small peptide, which was consistent with our recognition.[26] However, we believed that the evolution of the species obeyed the natural rules, thus inferring that the binding site could be composed of two or more known sites. Although the major topic of this work was analyzing the natural products, we also conducted virtual screening during the beginning months of the pandemic and reported the separation of the binding site as public information instead of a research paper. Sites I and II, respectively had the unique features of the previous CoV site and angiotensin receptor. This result was consistent with the clinical characteristics of SARS-CoV2.[11–13] Furthermore, some of the main components of Shuang and Lian were originally applied for inhibiting the similar sites.

Subsequently, the analysis of the prepared ligands in each binding site unveiled the substitutability of the herbs. Initially, Huang could be the supplement to the overall activity of Shuanghuanglian, and Huang could be de-emphasized considering the main bioactivity of the prescription. The herb resources of the selected hits are listed in Table S7. Among the 15 natural products, three were unique for Shuang and seven in Lian, hence inferring that these two herbs were irreplaceable. Several herbs also had five other hits and included *Chrysanthemi Flos* (359 compounds), *Aurantii Fructus Immaturus* (65 compounds), *Ginkgo Semen* (80 compounds), *Herbahypericiperforati* (37 compounds), *Canarii Fructus* (56 compounds), and *Saussureae Involucratae Herba* (55 compounds). These herbs could provide possible substitutability in urgent situations.

Conclusions

This study screened the potential binding of natural products in Shuanghuanglian to the the PLPro and Mpro of SARS-CoV2 by molecular docking simulation. There were 482 distinguished natural products in Shuanghuanglian that were categorized in the fatty acids, aromatic compounds, glycosides, and sterols. These compounds in these three herbs had certain repetition. The N3-binding site of the Mpro was further divided into five detailed sites. The successfully docked rates of the Shuanghuanglian components to these proteins were all higher than that of the compounds in the FDA-approved Drug Library. A majority of the top hits might interact with the binding sites via hydrogen bonds. In general, Shuang

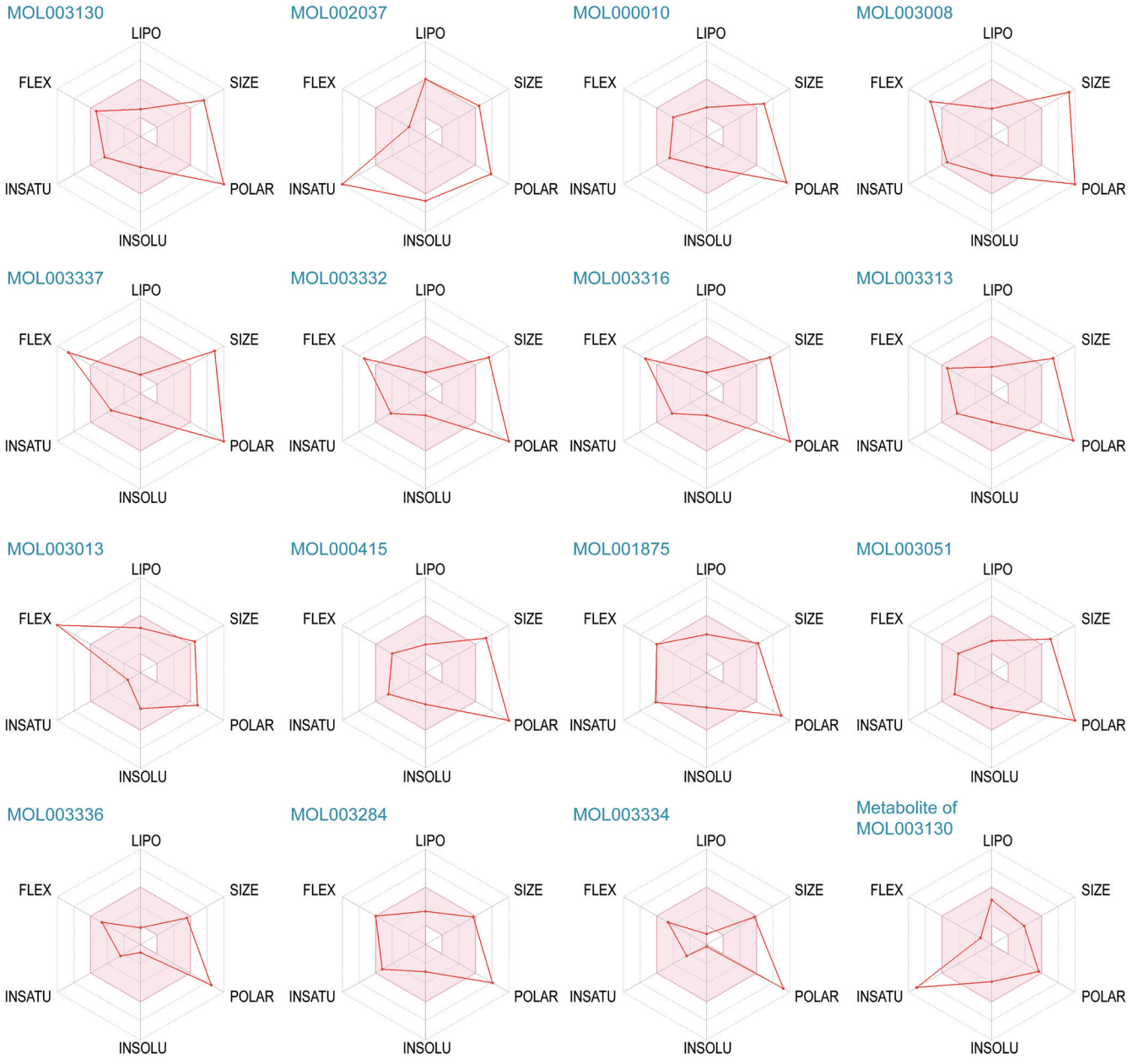

Fig. 6. The oral bioavailability radar maps of the selected hits and the metabolite of MOL003130. The colored zone was the suitable physiochemical space for oral bioavailability limited by LIPO (lipophility), SIZE, POLAR (polarity), INSO (insolubility), INSA (insaturation) and FLEX (flexibility).

and Lian took the primary status in providing the top hits, while Huang could act as an important supplement to their overall activity. Moreover, we checked the pharmacokinetic potential of the top hits. Though the selected hits faced the common difficulty of polarity, the deglycosylation and the package by the carriers could also be practical to overcome the violation. The substitutability of these herbs indicated that Shuang and Lian were irreplaceable, while other herbs seemed to have potential to be involved after further evaluation and analysis of the diversity and risks in the future. The findings from this work could open an avenue for international and standardized research on traditional Chinese medicines, thus contributing to global public health.

Supporting information

Supplementary material for this article is available at https://doi.org/10.14218/JERP.2022.00061.

Table S1. The natural products from the three major ingredients of Shuanghuanglian.

Table S2. The docked natural products which reached the basic requirement of potential interactions with SARS-CoV-2 PLPro (Ranked from left to right in each line).

Table S3. The docked natural products which reached the basic

requirement of potential interactions with SARS-CoV-2 Mpro N3-binding site (Ranked from left to right in each line).

Table S4. The top 50 hits in each binding site in SARS-CoV-2 Mpro.

Table S5. The predicted ADME properties of the selected hits and the Metabolite.

Table S6. The SMILE codes of the selected hits and the Metabolite.

Table S7. The herb resources of the selected hits.

Figure S1. The 2D binding patterns of the top 15 hits in SARS-CoV-2 PLPro.

Figure S2. The 2D binding patterns of the top 15 hits in SARS-CoV-2 Mpro at N3-binding site.

Figure S3. The 2D binding patterns of the top 15 hits in SARS-CoV-2 Mpro Site II.

Figure S4. The 2D binding patterns of the top 15 hits in SARS-CoV-2 Mpro Site III.

Figure S5. The 2D binding patterns of the top 15 hits in SARS-CoV-2 Mpro Site IV.

Figure S6. The 2D binding patterns of the top 15 hits in SARS-CoV-2 Mpro Site V.

Acknowledgments

We thank Prof. Yang Zhou and Dr. Peng-Fei Qi from Ningbo Institute of Materials Technology and Engineering, Chinese Academy of Sciences for their help in checking the parameters of the virtual screening.

Funding

This work was supported by the grants from the Innovation Fund for Technology of Nanjing University (2021), Research Project of Jinhua Traditional Chinese Medicine Science and Technology (2022KY33), and Scientific Research Project of Jinhua Advanced Research Institute (GYY202108 and GYY202104).

Conflict of interest

Yu-Shun Yang is a part-time academic consultant of Hi-Techjig Co. Ltd. (Zhenjiang, China). The authors have no other conflicts of interest to declare.

Author contributions

Conceptualization: YSY; formal analysis: YSY, DA, XW, and CYW; methodology: YSY and JY; writing the original draft: YSY; reviewing and editing: XW, CYW, and JY. All authors read and agreed to the published version of the manuscript.

Data sharing statement

The data from this study are available within the article and its supplementary files. Other corresponding details can be shared by requesting from the corresponding authors.

References

[1] Huang C, Wang Y, Li X, Ren L, Zhao J, Hu Y, *et al*. Clinical features of patients infected with 2019 novel coronavirus in Wuhan, China. Lancet 2020;395(10223):497–506. doi:10.1016/S0140-6736(20)30183-5, PMID:31986264.

[2] Li H, Liu L, Zhang D, Xu J, Dai H, Tang N, *et al*. SARS-CoV-2 and viral sepsis: observations and hypotheses. Lancet 2020;395(10235):1517–1520. doi:10.1016/S0140-6736(20)30920-X, PMID:32311318.

[3] van Doremalen N, Bushmaker T, Morris DH, Holbrook MG, Gamble A, Williamson BN, *et al*. Aerosol and Surface Stability of SARS-CoV-2 as Compared with SARS-CoV-1. N Engl J Med 2020;382(16):1564–1567. doi:10.1056/NEJMc2004973, PMID:32182409.

[4] de Groot RJ, Baker SC, Baric RS, Brown CS, Drosten C, Enjuanes L, *et al*. Middle East respiratory syndrome coronavirus (MERS-CoV): announcement of the Coronavirus Study Group. J Virol 2013;87(14):7790–7792. doi:10.1128/JVI.01244-13, PMID:23678167.

[5] Remuzzi A, Remuzzi G. COVID-19 and Italy: what next? Lancet 2020;395(10231):1225–1228. doi:10.1016/S0140-6736(20)30627-9, PMID:32178769.

[6] Bhatraju PK, Ghassemieh BJ, Nichols M, Kim R, Jerome KR, Nalla AK, *et al*. Covid-19 in Critically Ill Patients in the Seattle Region - Case Series. N Engl J Med 2020;382(21):2012–2022. doi:10.1056/NEJMoa2004500, PMID:32227758.

[7] Li R, Pei S, Chen B, Song Y, Zhang T, Yang W, *et al*. Substantial undocumented infection facilitates the rapid dissemination of novel coronavirus (SARS-CoV-2). Science 2020;368(6490):489–493. doi:10.1126/science.abb3221, PMID:32179701.

[8] Paules CI, Marston HD, Fauci AS. Coronavirus Infections-More Than Just the Common Cold. JAMA 2020;323(8):707–708. doi:10.1001/jama.2020.0757, PMID:31971553.

[9] Obermeyer F, Jankowiak M, Barkas N, Schaffner SF, Pyle JD, Yurkovetskiy L, *et al*. Analysis of 6.4 million SARS-CoV-2 genomes identifies mutations associated with fitness. Science 2022;376(6599):1327–1332. doi:10.1126/science.abm1208, PMID:35608456.

[10] Wilder-Smith A, Chiew CJ, Lee VJ. Can we contain the COVID-19 outbreak with the same measures as for SARS? Lancet Infect Dis 2020;20(5):e102–e107. doi:10.1016/S1473-3099(20)30129-8, PMID:32145768.

[11] Jiang S. Don't rush to deploy COVID-19 vaccines and drugs without sufficient safety guarantees. Nature 2020;579(7799):321. doi:10.1038/d41586-020-00751-9, PMID:32179860.

[12] Li G, De Clercq E. Therapeutic options for the 2019 novel coronavirus (2019-nCoV). Nat Rev Drug Discov 2020;19(3):149–150. doi:10.1038/d41573-020-00016-0, PMID:32127666.

[13] DeGrace MM, Ghedin E, Frieman MB, Krammer F, Grifoni A, Alisoltani A, *et al*. Defining the risk of SARS-CoV-2 variants on immune protection. Nature 2022;605(7911):640–652. doi:10.1038/s41586-022-04690-5, PMID:35361968.

[14] Xu X, Han M, Li T, Sun W, Wang D, Fu B, *et al*. Effective treatment of severe COVID-19 patients with tocilizumab. Proc Natl Acad Sci U S A 2020;117(20):10970–10975. doi:10.1073/pnas.2005615117, PMID:32350134.

[15] Shen C, Wang Z, Zhao F, Yang Y, Li J, Yuan J, *et al*. Treatment of 5 Critically Ill Patients With COVID-19 With Convalescent Plasma. JAMA 2020;323(16):1582–1589. doi:10.1001/jama.2020.4783, PMID:32219428.

[16] Wang M, Cao R, Zhang L, Yang X, Liu J, Xu M, *et al*. Remdesivir and chloroquine effectively inhibit the recently emerged novel coronavirus (2019-nCoV) in vitro. Cell Res 2020;30(3):269–271. doi:10.1038/s41422-020-0282-0, PMID:32020029.

[17] Du YX, Chen XP. Favipiravir: Pharmacokinetics and Concerns About Clinical Trials for 2019-nCoV Infection. Clin Pharmacol Ther 2020;108(2):242–247. doi:10.1002/cpt.1844, PMID:32246834.

[18] Gautret P, Lagier JC, Parola P, Hoang VT, Meddeb L, Mailhe M, *et al*. Hydroxychloroquine and azithromycin as a treatment of COVID-19: results of an open-label non-randomized clinical trial. Int J Antimicrob

Agents 2020;56(1):105949. doi:10.1016/j.ijantimicag.2020.105949, PMID:32205204.
[19] Sanders JM, Monogue ML, Jodlowski TZ, Cutrell JB. Pharmacologic Treatments for Coronavirus Disease 2019 (COVID-19): A Review. JAMA 2020;323(18):1824–1836. doi:10.1001/jama.2020.6019, PMID:32282022.
[20] Fernando K, Menon S, Jansen K, Naik P, Nucci G, Roberts J, *et al*. Achieving end-to-end success in the clinic: Pfizer's learnings on R&D productivity. Drug Discov Today 2022;27(3):697–704. doi:10.1016/j.drudis.2021.12.010, PMID:34922020.
[21] Hashemian SMR, Pourhanifeh MH, Hamblin MR, Shahrzad MK, Mirzaei H. RdRp inhibitors and COVID-19: Is molnupiravir a good option? Biomed Pharmacother 2022;146:112517. doi:10.1016/j.biopha.2021.112517, PMID:34902743.
[22] Mohamed Y, El-Maradny YA, Saleh AK, Nayl AA, El-Gendi H, El-Fakharany EM. A comprehensive insight into current control of COVID-19: Immunogenicity, vaccination, and treatment. Biomed Pharmacother 2022;153:113499. doi:10.1016/j.biopha.2022.113499, PMID:36076589.
[23] Zhu Z, Lu Z, Xu T, Chen C, Yang G, Zha T, *et al*. Arbidol monotherapy is superior to lopinavir/ritonavir in treating COVID-19. J Infect 2020;81(1):e21–e23. doi:10.1016/j.jinf.2020.03.060, PMID:32283143.
[24] Xiao M, Tian J, Zhou Y, Xu X, Min X, Lv Y, *et al*. Efficacy of Huoxiang Zhengqi dropping pills and Lianhua Qingwen granules in treatment of COVID-19: A randomized controlled trial. Pharmacol Res 2020;161:105126. doi:10.1016/j.phrs.2020.105126, PMID:32781283.
[25] Ni L, Zhou L, Zhou M, Zhao J, Wang DW. Combination of western medicine and Chinese traditional patent medicine in treating a family case of COVID-19. Front Med 2020;14(2):210–214. doi:10.1007/s11684-020-0757-x, PMID:32170559.
[26] Jin Z, Du X, Xu Y, Deng Y, Liu M, Zhao Y, *et al*. Structure of M^{pro} from SARS-CoV-2 and discovery of its inhibitors. Nature 2020;582(7811):289–293. doi:10.1038/s41586-020-2223-y, PMID:32272481.
[27] Shi Z, Liu Z, Liu C, Wu M, Su H, Ma X, *et al*. Spectrum-Effect Relationships Between Chemical Fingerprints and Antibacterial Effects of Lonicerae Japonicae Flos and Lonicerae Flos Base on UPLC and Microcalorimetry. Front Pharmacol 2016;7:12. doi:10.3389/fphar.2016.00012, PMID:26869929.
[28] Li C, Lin G, Zuo Z. Pharmacological effects and pharmacokinetics properties of Radix Scutellariae and its bioactive flavones. Biopharm Drug Dispos 2011;32(8):427–445. doi:10.1002/bdd.771, PMID:21928297.
[29] Jiao J, Fu YJ, Zu YG, Luo M, Wang W, Zhang L, *et al*. Enzyme-assisted microwave hydro-distillation essential oil from Fructus forsythia, chemical constituents, and its antimicrobial and antioxidant activities. Food Chem 2012;134(1):235–243. doi:10.1016/j.foodchem.2012.02.114.
[30] Zhou Z, Li X, Liu J, Dong L, Chen Q, Liu J, *et al*. Honeysuckle-encoded atypical microRNA2911 directly targets influenza A viruses. Cell Res 2015;25(1):39–49. doi:10.1038/cr.2014.130, PMID:25287280.
[31] Zhou LK, Zhou Z, Jiang XM, Zheng Y, Chen X, Fu Z, *et al*. Absorbed plant MIR2911 in honeysuckle decoction inhibits SARS-CoV-2 replication and accelerates the negative conversion of infected patients. Cell Discov 2020;6(1):54. doi:10.1038/s41421-020-00197-3, PMID:32802404.
[32] Zhou Z, Zhou Y, Jiang XM, Wang Y, Chen X, Xiao G, *et al*. Decreased HD-MIR2911 absorption in human subjects with the SIDT1 polymorphism fails to inhibit SARS-CoV-2 replication. Cell Discov 2020;6:63. doi:10.1038/s41421-020-00206-5, PMID:32934821.
[33] Ho LTF, Chan KKH, Chung VCH, Leung TH. Highlights of traditional Chinese medicine frontline expert advice in the China national guideline for COVID-19. Eur J Integr Med 2020;36:101116. doi:10.1016/j.eujim.2020.101116, PMID:32292529.
[34] Li Y, Li J, Zhong D, Zhang Y, Zhang Y, Guo Y, *et al*. Clinical practice guidelines and experts' consensuses of traditional Chinese herbal medicine for novel coronavirus (COVID-19): protocol of a systematic review. Syst Rev 2020;9(1):170. doi:10.1186/s13643-020-01432-4, PMID:32746913.
[35] Zhang D, Zhang B, Lv JT, Sa RN, Zhang XM, Lin ZJ. The clinical benefits of Chinese patent medicines against COVID-19 based on current evidence. Pharmacol Res 2020;157:104882. doi:10.1016/j.phrs.2020.104882, PMID:32380051.
[36] Qiu J. China plans to modernize traditional medicine. Nature 2007;446(7136):590–591. doi:10.1038/446590a, PMID:17410143.
[37] Leonti M, Casu L. Traditional medicines and globalization: current and future perspectives in ethnopharmacology. Front Pharmacol 2013;4:92. doi:10.3389/fphar.2013.0009, PMID:23898296.
[38] Li DD, Yu P, Xiao W, Wang ZZ, Zhao LG. Berberine: A Promising Natural Isoquinoline Alkaloid for the Development of Hypolipidemic Drugs. Curr Top Med Chem 2020;20(28):2634–2647. doi:10.2174/1568026620666200908165913, PMID:32901585.
[39] Ru J, Li P, Wang J, Zhou W, Li B, Huang C, *et al*. TCMSP: a database of systems pharmacology for drug discovery from herbal medicines. J Cheminform 2014;6:13. doi:10.1186/1758-2946-6-13, PMID:24735618.
[40] Ma C, Sacco MD, Xia Z, Lambrinidis G, Townsend JA, Hu Y, *et al*. Discovery of SARS-CoV-2 Papain-like Protease Inhibitors through a Combination of High-Throughput Screening and a FlipGFP-Based Reporter Assay. ACS Cent Sci 2021;7(7):1245–1260. doi:10.1021/acscentsci.1c00519, PMID:34341772.
[41] DeMirci H. Ambient-Temperature Serial Femtosecond X-ray Crystal structure of SARS-CoV-2 Main Protease at 2.1 A Resolution (P212121). doi:10.2210/pdb7cwc/pdb.
[42] Brooks BR, Bruccoleri RE, Olafson BD, States DJ, Swaminathan S, Karplus M. CHARMm - A program for macromolecular energy, minimization, and dynamics calculation. J Comput Chem 1983;4:187–217. doi:10.1002/jcc.540040211.
[43] Ratia K, Pegan S, Takayama J, Sleeman K, Coughlin M, Baliji S, *et al*. A noncovalent class of papain-like protease/deubiquitinase inhibitors blocks SARS virus replication. Proc Natl Acad Sci U S A 2008;105(42):16119–16124. doi:10.1073/pnas.0805240105, PMID:18852458.
[44] Wu G, Robertson DH, Brooks CL 3rd, Vieth M. Detailed analysis of grid-based molecular docking: A case study of CDOCKER-A CHARMm-based MD docking algorithm. J Comput Chem 2003;24(13):1549–1562. doi:10.1002/jcc.10306, PMID:12925999.
[45] Daina A, Michielin O, Zoete V. SwissADME: a free web tool to evaluate pharmacokinetics, drug-likeness and medicinal chemistry friendliness of small molecules. Sci Rep 2017;7:42717. doi:10.1038/srep42717, PMID:28256516.
[46] Daina A, Michielin O, Zoete V. iLOGP: a simple, robust, and efficient description of n-octanol/water partition coefficient for drug design using the GB/SA approach. J Chem Inf Model 2014;54(12):3284–3301. doi:10.1021/ci500467k, PMID:25382374.
[47] Lipinski CA, Lombardo F, Dominy BW, Feeney PJ. Experimental and computational approaches to estimate solubility and permeability in drug discovery and development settings. Adv Drug Deliv Rev 2001;46(1-3):3–26. doi:10.1016/s0169-409x(00)00129-0.
[48] Ertl P, Rohde B, Selzer P. Fast calculation of molecular polar surface area as a sum of fragment-based contributions and its application to the prediction of drug transport properties. J Med Chem 2000;43(20):3714–3717. doi:10.1021/jm000942e, PMID:11020286.
[49] Shen X, Yin F. The mechanisms and clinical application of Traditional Chinese Medicine Lianhua-Qingwen capsule. Biomed Pharmacother 2021;142:111998. doi:10.1016/j.biopha.2021.111998, PMID:34385103.
[50] Zhang L, Ma Y, Shi N, Tong L, Liu S, Ji X, *et al*. Effect of Qingfei Paidu decoction combined with Western medicine treatments for COVID-19: A systematic review and meta-analysis. Phytomedicine 2022;102:154166. doi:10.1016/j.phymed.2022.154166, PMID:35636170.